CHAOTIC BEHAVIOR OF A NEURAL NETWORK WITH DYNAMICAL THRESHOLDS

O. Hendin, D. Horn and M. Usher

School of Physics and Astronomy, Raymond and Beverly Sackler Faculty of Exact Sciences
Tel Aviv University, Tel Aviv 69978, Israel

Models of neural networks which include dynamical thresholds can display motion in pattern space, the space of all memories. We investigate this motion in a particular model which is based on a feedback network of excitatory and inhibitory neurons. We find that small variations in the parameters of the model can lead to big qualitative changes of its behavior. We display results of closed loops and chaotic motion which turn from one to the other through intermittency. We show that the basin of attraction of a closed orbit has a fractal shape, and find that the dimension of the chaotic motion is slightly bigger than 2. The general character of the dynamics of this model is convergence to centers of attraction on short time scales and divergence on long ones.

1. Introduction

Chaotic motion can be observed in neural networks with random and diluted asymmetric synaptic connections.[1,2,3] It is not expected to show up in attractor neural networks since these are highly stable systems which converge to fixed points. If, however, one introduces time dependence in the synaptic connections, the fixed points can be replaced by temporal sequences of patterns and chaotic motion may appear.[4] A recent study of analog neural networks with time delay[5] has shown that such systems display both periodic and chaotic motion. By changing the delay parameter, chaos is obtained via the route of period doubling.

We study a neural network with dynamical thresholds. The thresholds vary as a function of the activity of the neurons to which they are attached. As such they introduce time dependence which can turn a neural network from a dissipative system which converges onto fixed points into one which moves from one center of attraction to another.[6] This motion is the subject of our study. We will show the periodic and chaotic properties obtained by changing one parameter of our system, and demonstrate that the transition occurs through intermittency. We limit ourselves to a particular model which results in a set of differential equations for the order parameters of this system, the activities of the patterns. The model is briefly reviewed in the next section.

A system with p stored patterns (memories) is described in this model by $2p + 1$ differential equations in $2p + 1$ variables. These include the p activities which are the variables of interest. This system has three different kinds of behavior, depending on the values of the various parameters defining it. If the threshold effect is weak, the system will move into fixed points, like any other attractor neural network. When the thresholds are allowed to play an important role, one may obtain either a periodic motion or a chaotic one. In the latter case, the motion has a highest Lyapunov exponent which is positive, whereas in the former case the highest exponent is zero. Examples of this behavior are shown in Sec. 3, where we concentrate on the case of $p = 3$ memories. Although the number of patterns is small, the system is complicated enough to have all the intricate features of the general case. We shift from periodic to chaotic behavior by changing slowly one of the parameters and observe that this transition goes through intermittency. This is further substantiated in the next sections.

Section 4 is devoted to a particular case of $p = 3$, one which exhibits two kinds of periodic motion. We investigate the basins of attraction of these two limit cycles, and find them to have fractal boundaries. In Sec. 5, we study how the Lyapunov exponent is built up in the different regions of phase

space. We find that, in the neighborhood of the centers of attraction, it has clear negative contributions, whereas between them it gets very positive contributions. Thus we may characterize the motion as convergence to centers of attraction on short time scales and divergence on long time scales.

2. The Model

The system of equations which we will study comes from a model of excitatory and inhibitory neurons with dynamical thresholds.[7] The memory patterns are carried by the excitatory neurons only. Furthermore, we make the simplifying assumption that the patterns do not overlap with one another. This model can be thought of as having disjoint Hebbian cell assemblies of excitatory neurons which affect one another only through their interaction with a group of inhibitory neurons common to all of them. This allows one to represent the dynamics of a large number N of neurons in terms of a closed set of $p + 1$ differential equations, where p is the number of stored patterns.

Let us denote by $m^\mu(t)$ the fraction of the cell-assembly number μ which fires at time t, and by $m^I(t)$, the fraction of active inhibitory neurons. In a network with static thresholds, they obey the $p + 1$ equations

$$\frac{dm^\mu}{dt} = -m^\mu + F_T(Am^\mu - Bm^I - \theta^E) \quad (2.1)$$

$$\frac{dm^I}{dt} = -m^I + F_T(CM - Dm^I - \theta^I)$$

where

$$M = \sum_\mu m^\mu$$

and F_T is the sigmoid function

$$F_T(x) = (1 + e^{-x/T})^{-1} \quad (2.2)$$

depending on a temperature variable T which represents the noise in the system. θ^E and θ^I are the (constant) thresholds of all excitatory and inhibitory neurons correspondingly. The four parameters A, B, C and D are all positive and represent the different couplings between the neurons. A (which is normalized to 1 because of an overall arbitrary scale) is the interaction of any excitatory cell assem-

bly with itself and B is the effect of the inhibitory neurons on it. C is the effect of all excitatory neurons on the inhibitory ones, while D is their self-interaction. All stored patterns (or cell assemblies) are given the same weights in this description, and are therefore put on equal footing.

The differential equations (2.1) for the activities of the patterns obviously use continuous time. This is true even if the underlying neuron dynamics is described by discrete time due to the infinitesimal changes in the activities caused by the firing of any single neuron. Thus the dynamics of the excitatory neuron i which belongs to the cell assembly μ can be described by the equation

$$V_i^E(t + \Delta t) = f_T(h_i^E(t) - \theta_i^E(t))$$

$$h_i^E = Am^\mu - Bm^I ,$$

using the probabilistic rule

$$f_T(x) = \begin{cases} 1 \\ 0 \end{cases} \quad \text{with probability } (1 + e^{\mp x/T})^{-1}$$

$V_i^E(t)$ is a binary variable taking the value 1 if the E-neuron at location i fires at time t and 0 otherwise. Turning the thresholds of the excitatory neurons into dynamical variables we use the following relation,

$$\theta_i^E(t) = bR_i(t) + \theta_0^E$$

$$R_i(t + \Delta t) = \frac{R_i(t)}{c} + V_i^E(t + \Delta t) ,$$

where R_i is a local response function which leads to a variation of the threshold. Such a rule, for $c > 1$ and appropriate values of $g = bc/(c - 1)$; can exhibit local fatigue effects. The reason is simple. Imagine a situation in which, for a particular i, $V_i^E = 1$ for a long time period. In this case, the corresponding threshold will grow until it reaches $\theta_i^E = \theta^{max} = \theta_0^E + g$. If $\theta^{max} < h_i^E$ (the sum of post-synaptic potentials) this particular neuron will go on firing. However, in the case in which $\theta^{max} > h_i^E$, this cannot happen. As the threshold increases, it will stop the neuron from firing. Looking at the whole system of neurons we will observe a destabilization of the center of attraction at which the system finds itself. It will then move out of this

center and fall into the basin of attraction of a different center.

To incorporate this effect in the differential equations for the pattern activities, we introduce the variables

$$r^\mu = \frac{1}{N^\mu} \sum_{i \in \mu} R_i \qquad (2.6)$$

which measure the average response activity of pattern number μ. N^μ in this equation is the number of E-neurons which form the cell assembly of pattern number μ. We obtain then[7] the set of $2p + 1$ equations

$$\frac{dm^\mu}{dt} = -m^\mu + F_T(Am^\mu - Bm^I - \theta_0^E - br^\mu)$$

$$\frac{dr^\mu}{dt} = \left(\frac{1}{c} - 1\right) r^\mu + m^\mu \qquad (2.7)$$

$$\frac{dm^I}{dt} = -m^I + F_T(CM - Dm^I - \theta^I) \ .$$

Some of the general properties of these equations of motion can be deduced from the form of the function F_T.[7] We will concentrate here on the numerical investigation of their periodic and chaotic behavior.

3. Periodic Orbits, Chaotic Orbits and Intermittency

Let us investigate a series of cases of $p = 3$ which can be obtained by varying the inhibition parameter B while keeping all other parameters in the model fixed at the following values: $T = 0.1$, $A = 1$, $C = 1$, $D = 1.6$, $\theta_0^E = 0$, $\theta_0^I = 0.55$, $b = 0.085$, $c = 1.2$. The cases $B = 0.9$ and $B = 0.7$ were displayed in Ref. 2. They are examples of periodic and chaotic motion, respectively.

We represent our results in a two-dimensional plot whose axes are $x = m^3 - (m^1 + m^2)/2$, $y = \sqrt{3}(m^1 - m^2)/2$. The system has three centers of attraction which lie near $m^i = 1$ and form an equilateral triangle in this coordinate frame. In addition to these "pure" states there are also "mixed states", centers of attraction which correspond to pairwise equal activities, e.g., large $m^1 = m^2$ and small m^3. They form another equilateral triangle whose vertices lie on the diagonals of the first one. The relative importance of the two sets of centers of

attraction varies as a function of the parameters of the model.[7]

Figure 1 displays a set of trajectories for values of B starting with 0.6 and increasing by steps of 0.02 to 0.7. These figures show orbits which result from random initial conditions. The curves are drawn after some time is allowed for convergence into an asymptotic orbit. Measuring on these curves the highest Lyapunov exponent λ (see Sec. 5) we obtain the following results:

Table 1. Highest Lyapunov Exponent.

Figure	1a	1b	1c	1d	1e	1f
B	0.60	0.62	0.64	0.66	0.68	0.70
$\lambda(10^{-3})$	0.0	2	32	-1.5	1.2	24
Error(10^{-3})	0.5	1	5	0.5	0.6	4

Positive values should correspond to chaotic curves and zero values to periodic ones. Comparing Table 1 with the curves in Fig. 1, we see how this principle works. All cases which look chaotic have a Lyapunov exponent of order 10^{-2}. Such are Figs. 1c and 1f. In addition, we find marginal cases where, on the time scale we have been using, we observe creeping behavior which is in clear contrast with closed orbits of finite periodicity. These are the curves of Fig. 1b and 1e, whose Lyapunov exponents are positive but of order 10^{-3}. The curves which have a definite periodic structure, 1a and 1d, have a zero or a slightly negative exponent of order 10^{-3}.

The set of equations (2.7) is symmetric under the interchange of any two patterns. In the $p = 3$ case and the set of coordinates we use, this implies invariance under the reflection $y \to -y$ and rotation by 120°. Figure 1a is rotational invariant but slightly asymmetric under reflection. Its orbit has a definite chirality, and its motion is counterclockwise. There exists another orbit which is obtained through reflection and whose motion is clockwise. Figure 1b is invariant under reflection but not under rotation. It has almost closed loops with definite chiralities appearing in pairs. Clearly there exist other dynamical attractors which can be obtained by rotations of 120° for the same set of parameters. The chaotic motion of Fig. 1c seems to display all symmetries, while in the closed curve of Fig. 1d all are broken. Here again there is a definite chirality to the orbit, and five more copies can be generated through reflection and rotation.
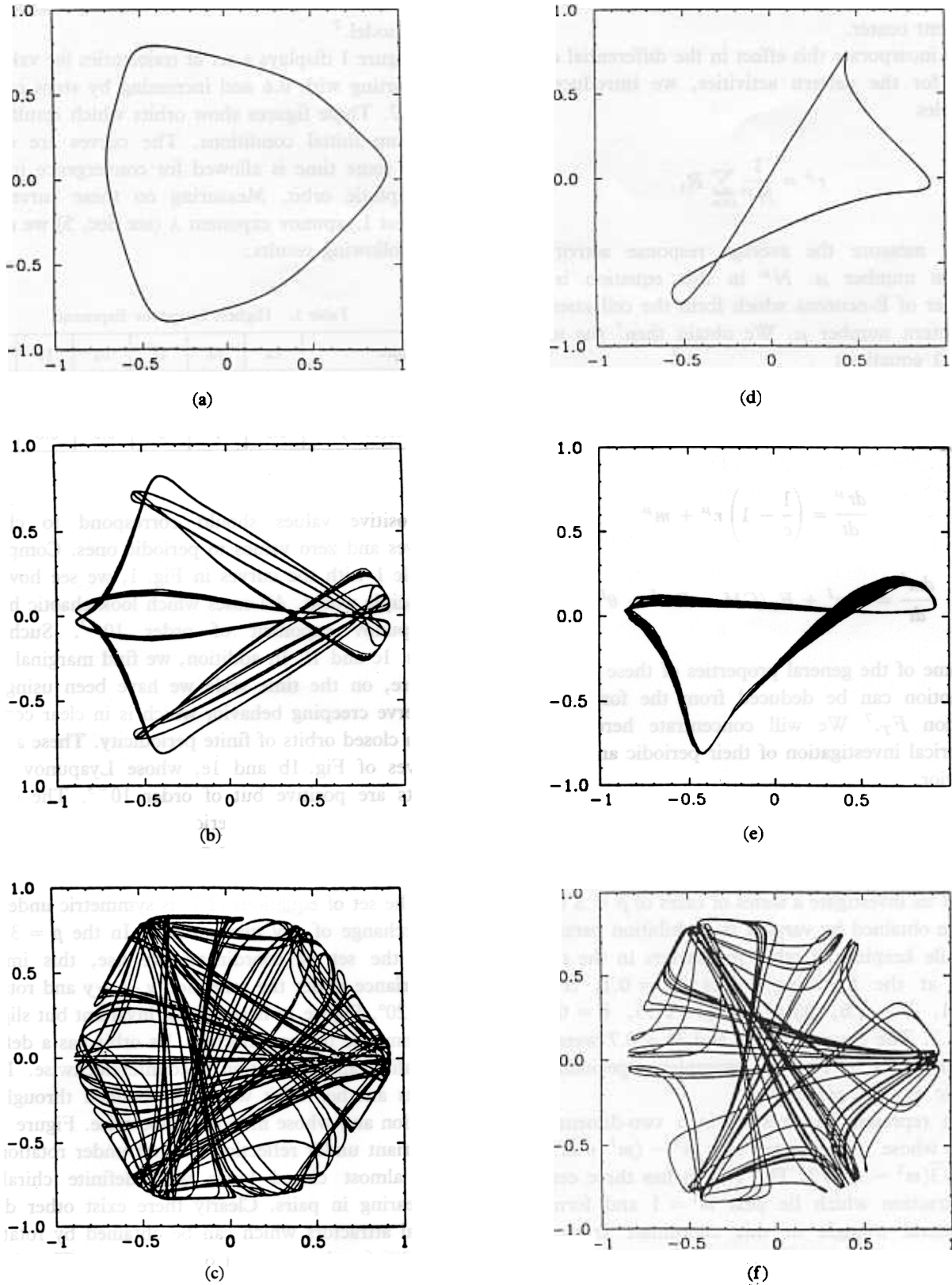
Fig. 1 Dynamical attractors plotted in the plane defined by $x = m^3 - (m^1 + m^2)/2$ and $y = \sqrt{3}(m^1 - m^2)/2$. All cases use the parameters $A = 1$, $C = 1$, $D = 1.6$, $T = 0.1$, $\theta^E = 0$, $\theta^I = 0.55$. They vary in the inhibition parameter B: (a) 0.60 (b) 0.62 (c) 0.64 (d) 0.66 (e) 0.68 (f) 0.70. Other attractors can be obtained through the symmetry operations discussed in the text.

The fact that the symmetry is restored in the chaotic case is no accident. It is quite easy to see how it comes about through intermittency: generation of chaotic motion through jumps between almost closed curves, in this case curves related by these symmetries. This is displayed in Fig. 2 whose value of the inhibition parameter is $B = 0.616$. This value of B lies in between those of Figs. 1a and 1b; yet the curve is not a closed one. The orbit starts in what seems to be an almost periodic curve which corresponds to a particular choice of symmetry breaking. It deviates continuously until it moves out of this quasi-periodic curve into another one which corresponds to a different choice of symmetry breaking. Eventually we obtain a symmetric structure which is built out of the three quasi-attractors.

It is conventional to study the approach to chaos by using a Poincaré map.[8] In Fig. 3 we display such a study of the case shown in Fig. 2. Plotted here are the results of a Poincaré map obtained when the orbit intersects the plane $m^3 = 0.5$. For each pair of consecutive points, we compare their values of $m^1 - m^2$, i.e., we plot y_n vs. y_{n-1}. We see that this map has two regions which are very close to the identity line, signifying the existence of two almost closed curves which intersect this plane. Starting at any of the extreme corners of this map, one flows into the region $y = 0$ and out of the quasi-attractor to be captured by the other quasi-attractor, and begin the motion at the other extreme corner. The points drawn on Fig. 3 correspond to one specific run through the two dynamic centers of attraction which cross the relevant plane. Repeating the process, one obtains points which are close, yet not identical, to the ones shown here. The new points lie in the same neighborhood and display the same trend. This is the trend which is typical of intermittency.

4. Fractal Basin of Attraction

There is a precursor to intermittency which can be observed in the case of periodic orbits. If there exist several different orbits, e.g., symmetry reflections of one another, one can study their basins of attraction. If the latter turn out to have fractal boundaries, this system may be expected to turn into intermittent motion after a small change in its parameters.

In this section, we study such a case. We choose the inhibition strength to be $B = 0.9$. This is a case where there exist two periodic orbits, corresponding
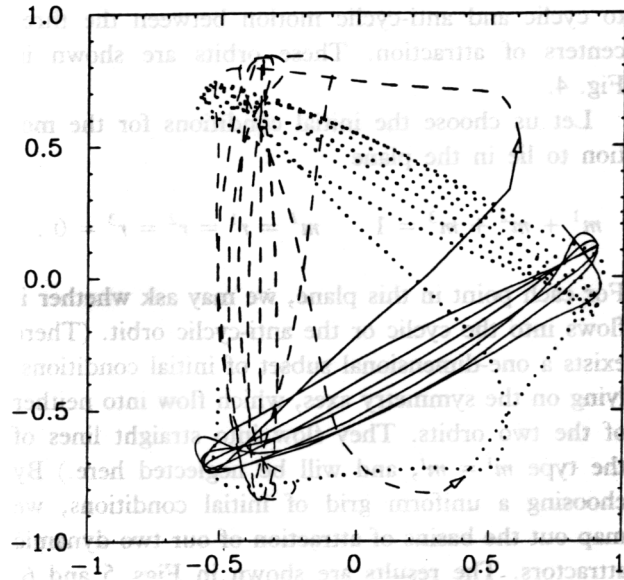

Fig. 2 A dynamical attractor which displays intermittency. Here, B was chosen as 0.616. We first observe an almost periodic curve drawn by a full line, which then moves into a rotated image drawn by a dashed line. The latter moves into the third image plotted by dots and so on.
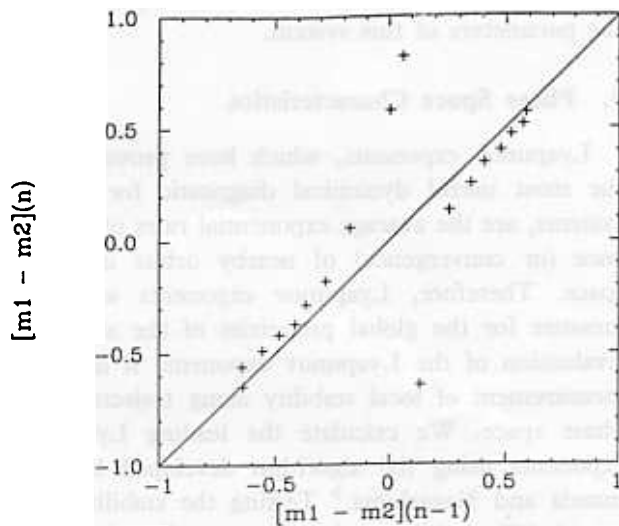

Fig. 3 A Poincaré map for the attractor displayed in Fig. 2. This map is drawn in the plane $m^3 = 1/2$, comparing the consecutive values of $m^1 - m^2$. The motion starts at the upper right corner, moves down to 0, then reappears in the lower left corner moving up to 1. The next cycle follows through nearby points which display the same trend. Although this represents only partial information of the orbit, it is enough to conclude that it has the character of intermittency.

to cyclic and anti-cyclic motion between the three centers of attraction. These orbits are shown in Fig. 4.

Let us choose the initial conditions for the motion to lie in the plane

$$m^1 + m^2 + m^3 = \qquad m^I = r^1 = r^2 = r^3 = 0 \;.$$

For each point in this plane, we may ask whether it flows into the cyclic or the anti-cyclic orbit. (There exists a one-dimensional subset of initial conditions, lying on the symmetry axes, which flow into neither of the two orbits. They flow into straight lines of the type $m^i = m^j$, and will be neglected here.) By choosing a uniform grid of initial conditions, we map out the basins of attraction of our two dynamic attractors. The results are shown in Figs. 5 and 6. We use the same x and y axes we employed before, this time to display the three-fold symmetry in the plane which we study. The black region corresponds to the basin of attraction of one orbit and the gray region to that of the other. Figure 6 is a blow-up of the right corner of Fig. 5. We learn from it that, as we go into finer scales, we uncover further boundaries between the two basins of attraction. They are therefore intertwined in a characteristic fractal manner, which is, as stated above, a precursor of the intermittent behavior observed for nearby choices of the parameters of this system.

Phase Space Characteristics

Lyapunov exponents, which have proven to be the most useful dynamical diagnostic for chaotic systems, are the average exponential rates of divergence (or convergence) of nearby orbits in phase space. Therefore, Lyapunov exponents supply a measure for the global properties of the attractor. Evaluation of the Lyapunov exponents is done by measurement of local stability along trajectories in phase space. We calculate the leading Lyapunov exponents using the algorithm developed by Shimanda and Nagashima.[9] Testing the stability of a set of differential equations, one studies the linearized set which follows for infinitesimal variations. Starting with a deviation vector V we will find, after time t, that its length becomes proportional to $2^{\lambda t}$ where λ is the highest Lyapunov exponent. This exponent is associated with the direction in tangent space which is growing most rapidly. Using a Gram–Schmidt procedure, one can obtain the lower exponents too.[9] In numerical evaluations, one starts
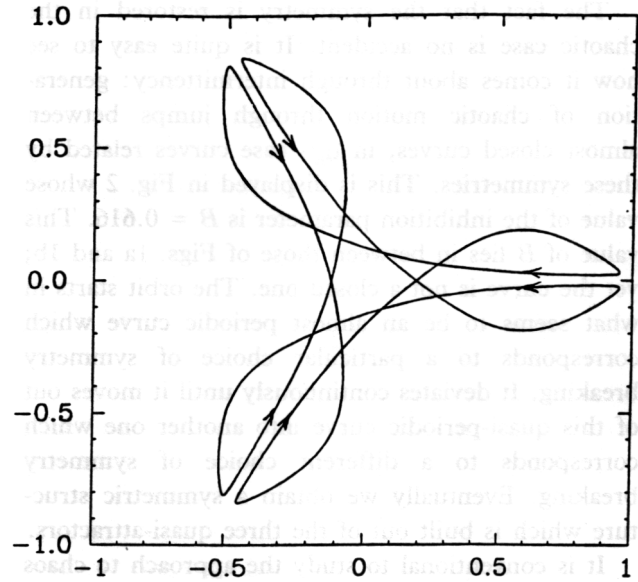

Fig. 4   The two mirror-image attractors which are obtained for $B = 0.9$. Their corners lie near the centers of attraction which correspond to the vertices of an equilateral triangle. The two attractors have opposite chiralities corresponding to cyclic or anti-cyclic motion.
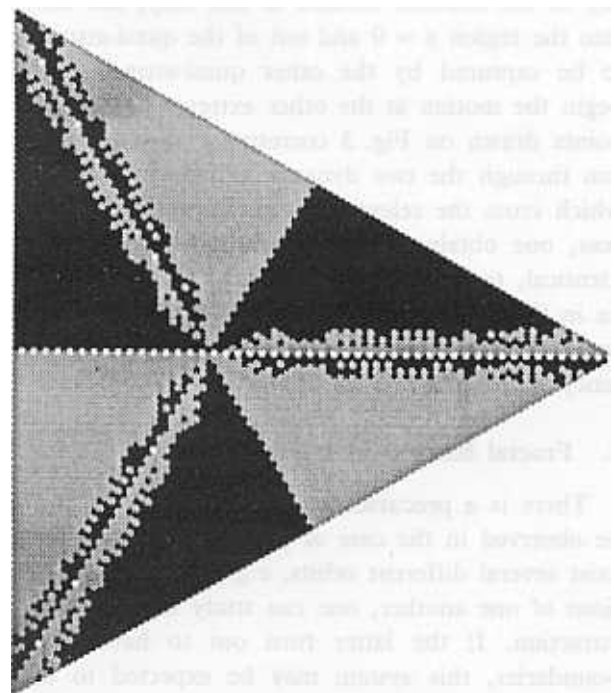

Fig. 5   Basins of attraction of the two dynamical attractors of Fig. 4 in the plane $m^1 + m^2 + m^3 = 1$ are plotted in two shades of gray. The border between the regions shows fractal behavior.

with one V whose norm is unity, lets it develop in time according to the linearized equations, and renormalizes it back to unity at time intervals which are not multiples of natural periods of the system. This breaks up the orbit into sections i in which the vectors develop until reaching values denoted by V_i, whose direction serves as the starting point for the next section. The leading exponent will then be

$$\lambda = \frac{\sum_i \ln |V_i|}{t \ln 2} \qquad (5.1)$$

where t is the total integration time, taken to be very long in order to obtain the asymptotic value.

In Fig. 7, we demonstrate this process by drawing the projections of the seven-dimensional vectors V_i on the x–y plane at the ends of each section for one run around the curve of Fig. 1a. Note the strong reduction in the size of the vectors near the centers of attraction. Clearly λ gets different contributions from different regions of phase space. To analyze this variation, let us introduce a radius $r^2 = x^2 + y^2$ and calculate separately contributions to λ which derive from sections which lie inside or outside a circle $r = R$. We define

$$\lambda_{\pm}(R) = \frac{\sum_{i \in R_{\pm}} \ln |V_i|}{t_{\pm} \ln 2} \qquad (5.2)$$

where $R_{\pm}$ are the regions $r > R$ and $r < R$, respectively, and $t_{\pm}$ is the time spent in them. It follows then that

$$\lambda = \frac{t_+ \lambda_+ + t_- \lambda_-}{t}. \qquad (5.3)$$

We have employed this procedure on the periodic case $B = 0.9$ (Fig. 4) and the chaotic case $B = 0.7$ (Fig. 1f). The results are shown in Fig. 8. Clearly large positive contributions to λ emerge from regions of low r values. Negative contributions come from high r regions where the centers of attraction are located. This agrees with the intuitive expectation that we see convergence near these centers and in the regions between them we have divergence. Since most of the time is spent near the centers of attraction, the small negative values can win over the large positive values. This is the case in the periodic curve of $B = 0.9$. The opposite holds for the chaotic curve of $B = 0.7$. The final λ values are seen at the edges, $R = 0$ and 1, of Fig. 8.
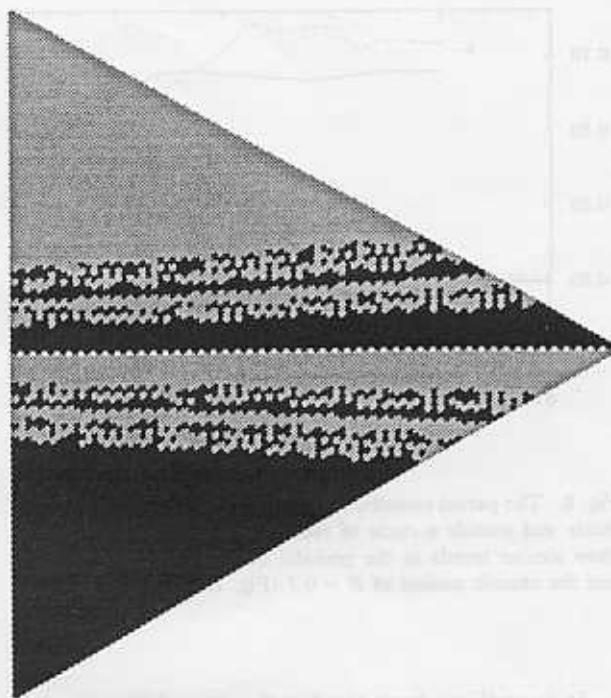

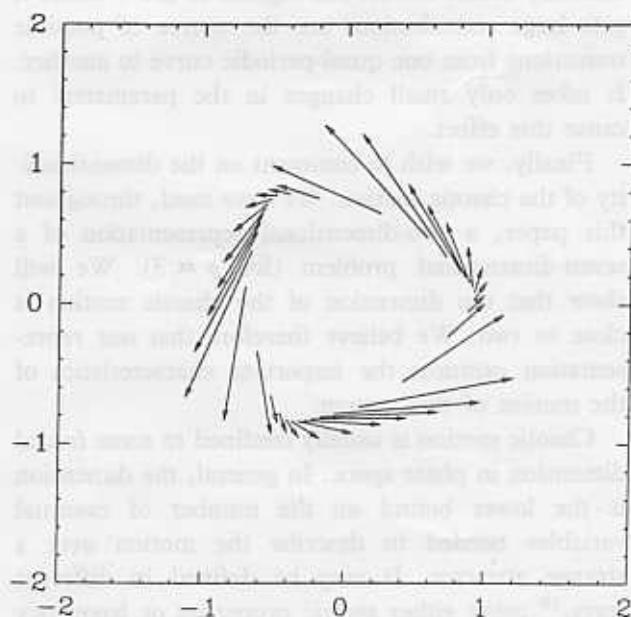Fig. 6 Blow-up of a corner of Fig. 5 substantiates the fractal structure.

Fig. 7 A set of vectors V_i for one cycle around the orbit of Fig. 1a. The vectors shown here are the two-dimensional projections of V_i. In order to obtain a clear demonstration of the trend of this system, we have started each section i with a vector of unit norm lying in the same plane, pointing along the direction of the projected V_{i-1}, i.e., along the direction of the vector seen in this figure.
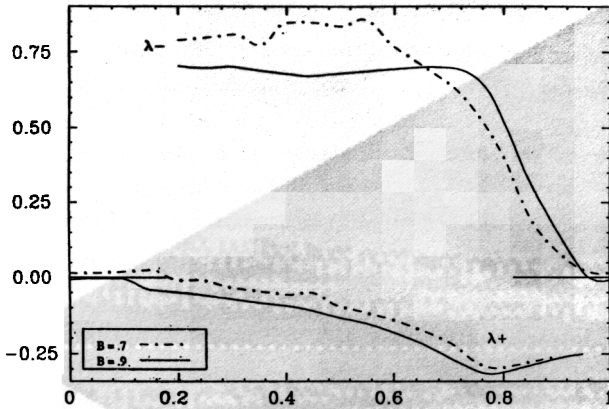
Fig. 8   The partial contributions to the Lyapunov exponent from inside and outside a circle of radius R, as defined in Eq. (5.2), show similar trends in the periodic motion of $B = 0.9$ (Fig. 4) and the chaotic motion of $B = 0.7$ (Fig. 1f).

It is striking how similar the two different cases look as a function of R and how delicate the balance between convergence and divergence seems to be. This explains how it is possible, by a small change in the parameters of the problem, to switch from periodic to chaotic behavior. It illustrates how intermittency comes about: the regions of low r where λ gets large contributions are the source of possible transitions from one quasi-periodic curve to another. It takes only small changes in the parameters to cause this effect.

Finally, we wish to comment on the dimensionality of the chaotic motion. We have used, throughout this paper, a two-dimensional representation of a seven-dimensional problem (for $p = 3$). We will show that the dimension of the chaotic motion is close to two. We believe therefore that our representation captures the important characteristics of the motion of this system.

Chaotic motion is usually confined to some fractal dimension in phase space. In general, the dimension is the lower bound on the number of essential variables needed to describe the motion over a strange attractor. It may be defined in different ways,[10] using either metric properties or frequency characteristics of the orbit.

In order to estimate the fractal dimension d_f of the set corresponding to $B = 0.7$, we used the definition of Kaplan and Yorke,[10] which relies on the Lyapunov exponents of the orbit. Ordering them in a descending order, starting from the highest $\lambda_1 > 0$ we have typically $\lambda_2 = 0$ and can

define the order j such that it is the first for which

$$\sum_{i=1}^{j} \lambda_i > 0 \qquad \sum_{i=1}^{j+1} \lambda_i < 0 \qquad (5.4)$$

Using this value j, Kaplan and Yorke defined the fractal dimension as

$$d_f = j + \frac{\sum_{i=1}^{j} \lambda_i}{|\lambda_{i+1}|} \qquad (5.5)$$

In the $B = 0.7$ case, we find that the value of the third exponent is -0.22, leading to $j = 2$ and $d_f = 2.15 \pm 0.03$ for this chaotic motion. Applying the same procedure to the case of $B = 0.64$, we obtain $d_f = 2.25 \pm 0.03$. All other cases depicted in Fig. 1 have dimensions close to 1. The two marginal cases of $B = 0.62$ (1b) and $B = 0.68$ (1e) lead to $d_f = 1.03 \pm 0.01$.

6.   Discussion

The model which we have investigated in this paper is defined by a set of differential equations for activities of excitatory and inhibitory cell assemblies. These equations can be justified within a specific neural network with a built-in fatigue effect caused by dynamical thresholds. The first numerical investigations of this model[7] have already indicated the existence of periodic and chaotic attractors. In this paper, we have investigated their properties in detail, and have shown that the transitions between periodic and chaotic behavior occurs via intermittency.

We have concentrated on a model with three stored patterns. We have fixed all parameters but for the inhibition strength B, which was tuned carefully so as to reveal different kinds of orbits. Examples were shown in Fig. 1. To put things in perspective we display in Fig. 9 the Lyapunov exponents measured by sweeping over the parameter B with steps of 0.001. The choices of Fig. 1, whose Lyapunov exponents were quoted in Table 1, are indicated by circles on Fig. 9. We see that they belong to a range of B which has very strong variations in behavior. Moreover, the values of the positive Lyapunov exponents which indicate chaotic behavior are very small. To understand these small differences between periodic and chaotic trajectories, we have developed a method which measures semi-local properties of the Lyapunov exponents. Evaluating the contributions to the leading Lyapunov
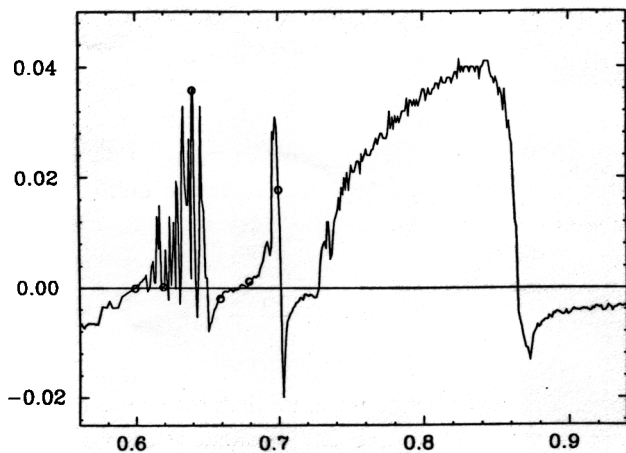
Fig. 9 Variation of the highest Lyapunov exponent λ as a function of the parameter B using a step size of 0.001. The six cases displayed in Fig. 1 and evaluated in Table 1 are indicated by small circles.

exponent from different regions in phase space, we have seen that in both cases we obtain large negative contributions in the neighborhood of the centers of attraction, and large positive values in the regions which are far away from these centers. A very delicate balance between these two components determines whether the resulting orbit is a periodic, quasi-periodic or chaotic one. The first component describes short-term convergence to centers of attraction, while the second one represents the destabilizing effects of the dynamical thresholds. In the chaotic case, the latter wins, leading to long-term divergence.

Intermittency can be understood in terms of this delicate balance between attraction and repulsion. Small changes in the parameters can easily spoil the balance and turn a periodic structure into a pseudo-periodic one, which almost closes on itself. The trajectory can then easily move from the neighborhood of one periodic curve to another, exhibiting intermittency. An example was shown in Fig. 2. Another indication of this tendency is given by the fractal basins of attraction of the periodic attractors shown in Fig. 5.

All these quantitative and qualitative arguments help to establish the general nature of the dynamics of our model. This model is not intended to describe any specific neural system, but it is supposed to serve as an example of a neural system which is able to move freely (i.e., unpredictably) within its set of stored patterns. Chaos is the technical definition of this freedom: the long-term divergence of

this system comes about through its crucial dependence on initial conditions which are buried in the microscopic details of the model. Judging only by its measurable amplitudes (the activities of the stored patterns) its behavior is unpredictable. We believe that this property deserves attention. Future neural models of thought processes will undoubtedly make extensive use of chaotic features in order to account for the apparent freedom of the brain.

Acknowledgment

References

1. H. Sompolinsky and A. Crisanti, "Chaos in random neural networks", *Phys. Rev. Lett.* **61** (1988) 259–262.
2. K. E. Kurten, "Critical phenomena in model neural networks", *Phys. Lett.* **A129** (1988) 157–160.
3. M. Bauer and W. Martienssen, "Quasi-periodicity route to chaos in neural networks", *Europhys. Lett.* **10** (1989) 427–431.
4. U. Riedel, R. Kuhn and J. L. van Hemmen, "Temporal sequences and chaos in neural nets", *Phys. Rev.* **A38** (1987) 1105–1108.
5. C. M. Marcus and R. M. Wetervelt, "Dynamics of analog neural-networks with time delay", in *Advances in Neural Information Processing Systems* (Morgan Kauffman, San Mateo CA, 1989).
6. D. Horn and M. Usher, "Neural networks with dynamical thresholds", *Phys. Rev.* **A40** (1989) 1036–1044.
7. D. Horn and M. Usher, "Excitatory–inhibitory networks with dynamical thresholds", *Int. J. Neural Systems* **1** (1990) 249–257.
8. Y. Pomeau and P. Manneville, "Intermittent transition to turbulence in dissipative dynamical systems", *Comm. Math. Phys.* **74** (1980) 189–197.
9. I. Shimanda and T. Nagashima, "A numerical approach to ergodic problem of dissipative dynamical systems", *Prog. Theor. Phys.* **61** (1979) 1605–1615.
10. J. D. Farmer, E. Ott and J. A. Yorke, "The dimension of chaotic attractors", *Physica* **7D** (1983) 153–180.